Check for updates

Received: 28 March 2022 | Revised: 12 August 2022 | Accepted: 23 August 2022

DOI: 10.1111/cas.15565

Cancer Science WILEY

ORIGINAL ARTICLE

Pathological complete remission of relapsed tumor by photo-activating antibody–mimetic drug conjugate treatment

Yudai Kaneko[1,2] | Kenzo Yamatsugu[3] | Takefumi Yamashita[1] | Kazuki Takahashi[3] | Toshiya Tanaka[1] | Sho Aki[1] | Toshifumi Tatsumi[3] | Takeshi Kawamura[1,4] | Mai Miura[1] | Masazumi Ishii[1] | Kei Ohkubo[5,6] | Tsuyoshi Osawa[1] | Tatsuhiko Kodama[1] | Shumpei Ishikawa[7] | Masanobu Tsukagoshi[8] | Michael Chansler[8] | Akira Sugiyama[1,4] | Motomu Kanai[3] | Hiroto Katoh[7]

[1]Research Center for Advanced Science and Technology, The University of Tokyo, Tokyo, Japan

[2]Medical & Biological Laboratories Co., Ltd, Tokyo, Japan

[3]Graduate School of Pharmaceutical Sciences, The University of Tokyo, Tokyo, Japan

[4]Isotope Science Center, The University of Tokyo, Tokyo, Japan

[5]Institute for Open and Transdisciplinary Research Initiatives, Osaka University, Osaka, Japan

[6]Institute for Advanced Co-Creation Studies, Osaka University, Osaka, Japan

[7]Department of Preventive Medicine, Graduate School of Medicine, The University of Tokyo, Tokyo, Japan

[8]Savid Therapeutics Inc., Tokyo, Japan

Correspondence
Akira Sugiyama, Research Center for Advanced Science and Technology, The University of Tokyo, 4-6-1 Komaba, Meguro-ku, Tokyo 153-8904, Japan.
Email: sugiyama@lsbm.org

Motomu Kanai, Laboratory of Synthetic Organic Chemistry, Graduate School of Pharmaceutical Sciences, The University of Tokyo, 7-3-1, Hongo, Bunkyo-ku, Tokyo 113-0033, Japan.
Email: kanai@mol.f.u-tokyo.ac.jp

Hiroto Katoh, Department of Preventive Medicine, Graduate School of Medicine, The University of Tokyo, 7-3-1 Hongo, Bunkyo-ku, Tokyo, 113-0033 Japan.
Email: hkat-prm@m.u-tokyo.ac.jp

Funding information
Japan Society for the Promotion of Science, Grant/Award Number: JP21392851; Kowa Life Science Foundation; Program for Promoting Researches on the Supercomputer Fugaku, Grant/Award Number:

Abstract

Antibody–mimetic drug conjugate is a novel noncovalent conjugate consisting of an antibody-mimetic recognizing a target molecule on the cancer cell surface and low-molecular-weight payloads that kill the cancer cells. In this study, the efficacy of a photo-activating antibody–mimetic drug conjugate targeting HER2-expressing tumors was evaluated in mice, by using the affibody that recognize HER2 ($Z_{HER2:342}$) as a target molecule and an axially substituted silicon phthalocyanine (a novel potent photo-activating compound) as a payload. The first treatment with the photo-activating antibody–mimetic drug conjugates reduced the size of all HER2-expressing KPL-4 xenograft tumors macroscopically. However, during the observation period, relapsed tumors gradually appeared in approximately 50% of the animals. To evaluate the efficacy of repeated antibody–mimetic drug conjugate treatment, animals with relapsed tumors were treated again with the same regimen. After the second observation period, the mouse tissues were examined histopathologically. Unexpectedly, all relapsed tumors were eradicated, and all animals were diagnosed with pathological complete remission. After the second treatment, skin wounds healed rapidly, and no significant side effects were observed in other organs, except for occasional

Abbreviations: ADC, antibody-drug conjugate; AMDC, antibody–mimetic drug conjugate; Ax-SiPc, axially substituted silicon phthalocyanine; EGFR, epidermal growth factor receptor; HER2, human epidermal growth factor receptor 2; IB, inclusion body.

This is an open access article under the terms of the Creative Commons Attribution-NonCommercial License, which permits use, distribution and reproduction in any medium, provided the original work is properly cited and is not used for commercial purposes.
© 2022 The Authors. *Cancer Science* published by John Wiley & Sons Australia, Ltd on behalf of Japanese Cancer Association.

JPMXP1020200201 and hp210172; Savid Therapeutics, Inc.; Takeda Science Foundation; the Japan Agency for Medical Research and Development, Grant/Award Number: JP20ck0106414, JP21am0401010 and JP21ak0101096

microscopic granulomatous tissues beneath the serosa of the liver in a few mice. Repeated treatments seemed to be well tolerated. These results indicate the promising efficacy of the repeated photo-activating antibody–mimetic drug conjugate treatment against HER2-expressing tumors.

KEYWORDS
antibody–mimetic drug conjugate, HER2, pathological complete remission, photoimmunotherapy, silicon phthalocyanine

1 | INTRODUCTION

An emerging concept in cancer therapy is antibody-drug conjugates (ADCs), which are monoclonal antibodies linked to cytotoxic payloads.[1] Owing to the highly selective behavior of ADCs in delivering potent cytotoxic drugs to tumor cells in xenograft models, they are developed as a part of targeted therapies to expand the therapeutic window and reduce the adverse effects.[2,3] Recently, more than ten cancer therapeutic drugs, such as gemtuzumab ozogamicin (Mylotarg®) and brentuximab vedotin (Adcetris®), were approved by the US Food and Drug Administration and many ADC candidates still are subjected to clinical studies, which suggests the success of the ADC strategy for cancer therapy.[4,5]

Concurrently with the development of antibody drugs, some studies report the design and development of a wide variety of antibody mimetics.[6–8] Recent advances in the protein computational design enabled the systematic development of antibody-mimetic,[9,10] which has great potential for new therapeutic agents like ADCs.

In this study, we have reported the development of a new therapeutic concept for cancer therapy, antibody–mimetic drug conjugates (AMDCs), using the modified streptavidin-biotin system.[11,12] Based on the strong noncovalent binding of streptavidin and biotin, a Cupid (mutated low-immunogenic streptavidin protein) and Psyche (modified biotin) system have been developed.[12] Furthermore, we have developed an axially substituted silicon phthalocyanine (Ax-SiPc), a potent photosensitizer, conjugated to Psyche as a payload.[13] In a previous study, a powerful photo-activating anti-HER2 AMDC was developed by combining a high-affinity anti-HER2 antibody–mimetic, $Z_{HER2:342}$,[14] fused to Cupid, with Psyche binding to Ax-SiPc. $Z_{HER2:342}$ and Cupid were not antigenic in primates.[12,15] Furthermore, this drug showed a marked tumor-reducing effect against KPL-4 xenografts, a human HER2-expressed breast cancer cell line, without side effects.[11] However, pathological analysis after the initial treatment indicated that some animals had malignant cells in their remains.[11] This result raised concerns about the efficacy of the single treatment by AMDCs using the photosensitizer.

The long-term effects of current standard therapy are limited by recurrent tumors and the development of resistance to drugs.[16] Malignant cells that are resistant to cytotoxic drugs develop into refractory tumors.[17–19] To overcome the development of drug resistance, photoimmunotherapy has recently been developed using the photosensitizer IR700 as a payload conjugated to an epidermal growth factor receptor (EGFR) antibody.[20] This treatment created a rapid and potent killing effect on EGFR-expressing malignant cells. Clinical trials on head and neck cancers are in progress worldwide.[21] Due to its physicochemical mechanism and additional induction of tumor immunity, it may be difficult for cancer cells to develop resistance to AMDC therapy.[22]

Here, we are reporting the details of animal experimental results under carefully selected conditions to evaluate the efficacy of repeated photo-activating AMDCs against relapsing xenograft tumors. A series of animal experiments were conducted to assess the repeated AMDC treatments.

2 | MATERIALS AND METHODS

2.1 | Reagents and chemicals

Escherichia coli strain BL21(DE3) (catalog number: 312–06534, Nippon Gene) was used as an expression host. The pET-45b(+) vector was used for cloning and gene expression analysis (catalog number: 71327; Novagen). The denaturation buffer consisted of 0.1 M Tris-HCl, pH 8.5, 10 mM EDTA, and 6 M guanidine hydrochloride. The refolding buffer consisted of 0.1 M sodium phosphate and 0.4 M arginine-HCl, pH 6.0. The gel filtration buffer consisted of 0.1 M sodium phosphate and 0.2 M arginine-HCl, pH 6.5. The photosensitizer, Psyche-Ax-SiPc, was provided by Prof. Kanai's laboratory at the University of Tokyo.[11,13] Human breast cancer KPL-4 cells were a generous gift from Prof. Kurebayashi (Kawasaki Medical School). Kadcyla® (trastuzumab emtansine) was purchased from Roche.

2.2 | Preparation of recombinant $Z_{HER2:342}$-Cupid-His

The recombinant $Z_{HER2:342}$-Cupid-His protein was manufactured from *Escherichia coli* inclusion bodies (IBs) by denaturalization using a denaturant and a direct dilution refolding method. The details of the expression and purification of the recombinant $Z_{HER2:342}$-Cupid-His protein have been previously described.[12] Briefly, *Escherichia coli* strain BL21(DE3) was transformed with the expression vector pET45b(+)-$Z_{HER2:342}$-Cupid-His and expressed recombinant $Z_{HER2:342}$-Cupid-His protein as IBs. Purified IBs were solubilized in

the denaturation buffer. The solubilized IB solution was clarified using centrifugation (12,000*g*, 15 minutes at 4°C) and refolded using a direct 40-fold dilution with refolding buffer. After 72 hours of incubation at 4°C, the refolded tetrameric recombinant $Z_{HER2:342}$-Cupid-His protein was purified with gel filtration buffer using a gel filtration column (HiLoad 16/600 Superdex 75 pg, #28989333, Cytiva).

2.3 | In vivo breast cancer tumor model experiment

2.3.1 | Approval of animal study

This study was approved by the Institutional Animal Care and Use Committee (approval number: RAC210005) and carried out according to the animal experimentation regulations of the University of Tokyo.

2.3.2 | Preparation of animal models

The KPL-4 cell line was maintained in DMEM (low glucose) (FUJIFILM Wako Pure Chemical Corporation) supplemented with 10% FBS, 100 U ml^{-1} penicillin, and 100 μg ml^{-1} streptomycin (#15140122, Thermo Fisher Scientific).[23] KPL-4 cells (7.5 million) were transplanted subcutaneously into the thigh of BALB/cSlc-nu/nu nude mice (Sankyo Labo Service Corporation, Inc.). Subcutaneous tumor growth was monitored by measuring tumor volume ($0.5 \times length \times width^2$) using a caliper, and the animal body weight was monitored as an indicator of treatment-related toxicity. The tumor size in 20 mice increased 44 days after cell implantation, reaching approximately 400 mm^3. These 20 mice were randomly divided into two groups of 10 mice each, the Kadcyla® group and the $Z_{HER2:342}$-Cupid-His-Ax-SiPc group.

2.3.3 | In vivo experimental design

Kadcyla®, the anti-Her2 ADC, was used as a control to confirm that administration experiments in the KPL-4 xenograft mice were performed properly. $Z_{HER2:342}$-Cupid-His-Ax-SiPc (Figure 1A) was injected into the xenograft model mice on day 0. Yamatsugu et al. reported that there were no visible tumors in any of the xenograft model mice on day 19 after $Z_{HER2:342}$-Cupid-His-Ax-SiPc injection; however, a small cluster of tumor cells in the fibrous skin persisted in one of the model mice on histopathological examination.[11] In this study, the observation period was determined to be approximately 19 days after the first treatment to assess tumor relapse. In case of tumor relapse, the second treatment was administered 44 days after the recurrence check period (day 63 after the first treatment) for cancer cell growth, the same period before the first treatment.

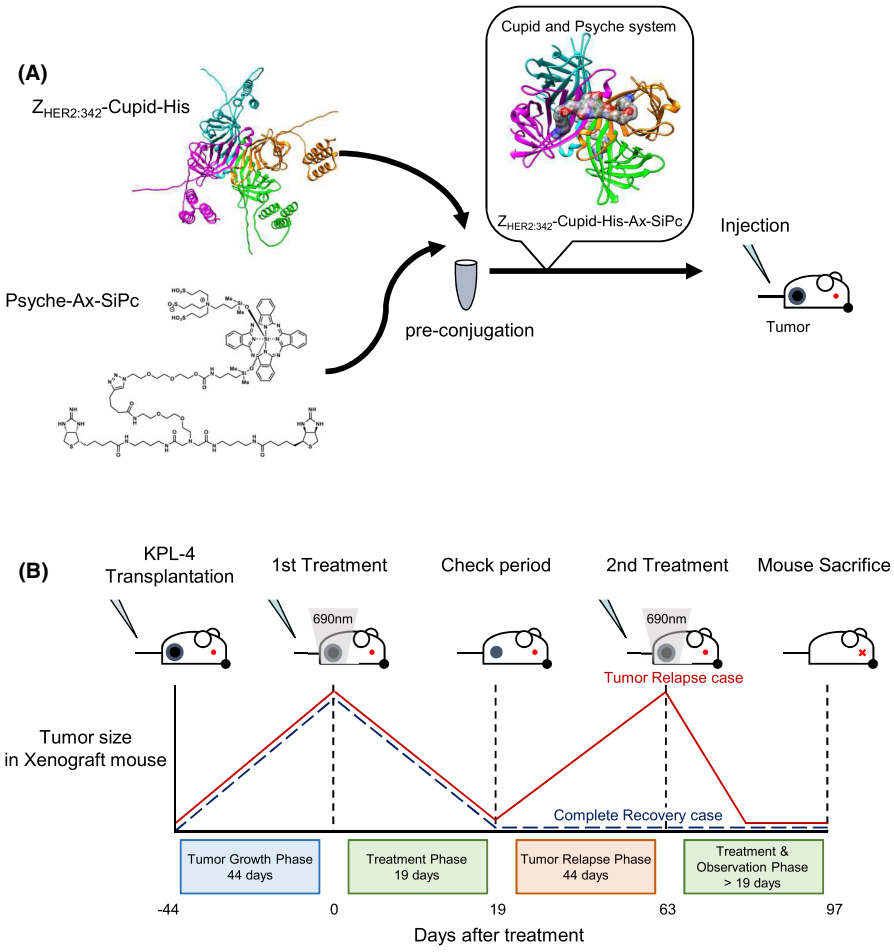

FIGURE 1 Strategy of the $Z_{HER2:342}$-Cupid-His-Ax-SiPc treatment for HER2-positive breast cancer. (A) Schematic explanation for the pre-conjugation of the $Z_{HER2:342}$-Cupid-His and Psyche-Ax-SiPc. (B) Experimental timeline of the xenograft model mice

Finally, the xenograft model mice were sacrificed on day 97 after the treatment and more than 19 days after the second treatment. Figure 1B shows a graphical overview of the experimental design.

2.3.4 | Preparation of treatment drugs

Local treatment with $Z_{HER2:\ 342}$-Cupid-His-Ax-SiPc has been reported.[11] Kadcyla® was used as a whole-body treatment model.[24] Kadcyla® was prepared according to the manufacturer's instructions. A previous report provided detailed information on the preparation of $Z_{HER2:342}$-Cupid-His and Psyche-Ax-SiPc.[11] Briefly, Psyche-Ax-SiPc solubilized in dimethyl sulfoxide at a concentration of 5 mM was stored at −80°C as a stock solution. To induce complex formation, $Z_{HER2:342}$-Cupid-His and Psyche-Ax-SiPc were mixed in a molar ratio of 1:2 in the dark on ice for 10 minutes. The concentration of $Z_{HER2:342}$-Cupid-His-Ax-SiPc was diluted using phosphate-buffered saline.

2.3.5 | Treatment of model mice

Kadcyla® and $Z_{HER2:342}$-Cupid-His-Ax-SiPc were administered at 300 μg[24] and 150 μg[11]. Twenty hours after injection, the $Z_{HER2:342}$-Cupid-His-Ax-SiPc group mice were irradiated with 690 nm light-emitting diode light (Yamato Scientific Co., Ltd.) at 230 J cm^{-2} under anesthesia. Forty-eight hours after the first light irradiation, the tumors were irradiated again in the same manner.

2.3.6 | Pathological analysis

Skin samples from the xenografted tumor sites and other vital organs, including the lung, heart, kidney, liver, and alimentary tracts, were obtained from the mice, fixed with 4% paraformaldehyde phosphate buffer solution (#163–20,145, FUJIFILM Wako Pure Chemical Corporation [FUJIFILM]) for 24 hours at 4°C, and embedded in paraffin. The histopathological specimens were deparaffinized by immersion in xylene (#241–00091, FUJIFILM) for 10 minutes at room temperature, and rehydrated by immersion in ethanol (#057–00451, FUJIFILM). Hematoxylin (#6187-4P, Sakura Finetek) and eosin (#8660, Sakura Finetek) were used for H&E staining following the manufacturer's protocols. The stained slides were dehydrated by immersion in ethanol followed by xylene. Glass coverslips with Marinol (#4197193; Muto Pure Chemicals) were used to cover the stained slides. H&E-stained slides were examined using OLYMPUS cellSens Standard system (OLYMPUS).

2.3.7 | Statistical analysis

P value <0.05 ($p<0.05$) was considered statistically significant. All graphs, calculations, and statistical analyses were performed using the statistical package for Microsoft Excel (Microsoft Corp.).

Other materials and methods are available in the supporting information (Appendix S1).

3 | RESULTS

3.1 | Local AMDC treatment reduced tumor volume in xenograft mouse model rapidly but led to relapse in some cases

For the purpose of establishing a HER2-positive breast cancer mouse xenograft model, we subcutaneously transplanted KPL-4 cells into BALB/cSlc-nu/nu nude mice. We mixed $Z_{HER2:342}$-Cupid-His and Psyche-Ax-SiPc in order to induce AMDC complex formation. This mixture after the irradiation resulted in the production of singlet oxygen detected by phosphorescence emission at 1270 nm, which was thought to induce cell death[20] and confirmed to achieve tumor necrosis in our in vivo model (Figure S1). It was also confirmed that the AMDC showed clear effects on HER2-overexpressing cells including KPL-4 in vitro (Figure S2). The tumor volume in 20 mice increased after KPL-4 cell injection and reached a mean volume of $400 \pm 110\ mm^3$ (from 125 to 551 mm^3) 44 days after cell transplantation. The KPL-4 xenograft model mice were randomly divided into two treatment groups ($n = 10$ per group): Kadcyla® was injected on day 0 in group 1 (mean ± SD: 417 ± 88), and $Z_{HER2:342}$-Cupid-His-Ax-SiPc was injected on day 0 in group 2 (mean ± SD: 384 ± 126). Both groups were irradiated on day 1 (24-hour interval after injection) and day 3 (72-hour interval after injection). No statistically significant difference was noted between the tumor volumes in each mouse in the Kadcyla® and $Z_{HER2:342}$-Cupid-His-Ax-SiPc groups.

For the evaluation of the effects of local AMDC therapy, we measured chronological changes in tumor volume in KPL-4 xenograft model mice after Kadcyla® and $Z_{HER2:342}$-Cupid-His-Ax-SiPc treatment. Figure 2 shows the change in tumor volume in KPL-4 xenograft model mice after Kadcyla® and $Z_{HER2:342}$-Cupid-His-Ax-SiPc injection. In both groups, a decrease in tumor size was observed after the first treatment. There was a significant difference in the reduction of tumor volume between the Kadcyla® and $Z_{HER2:342}$-Cupid-His-Ax-SiPc groups in the early stage: day 4 ($p<0.001$), day 7 ($p<0.001$), day 11 ($p<0.001$), day 14 ($p<0.01$), and day 17 ($p<0.05$) after the treatment (Figure 2A). The tumor volumes in the KPL-4 xenograft model mice decreased slowly after Kadcyla® treatment, being reduced to 0 mm^3 in only one case 21 days after the injection (Figure 2B,D), whereas the tumor size in the same xenograft model decreased rapidly after $Z_{HER2:342}$-Cupid-His-Ax-SiPc treatment. Further, tumor in approximately half of the mice disappeared on day 11 after $Z_{HER2:342}$-Cupid-His-Ax-SiPc injection (Figure 2C,D). The mean tumor volume was the smallest around day 20 after treatment and during the recurrence check period. However, in the observation period, the tumor volume in the xenograft model mice persisted and gradually increased in size again in 5/10 cases. In some cases, the tumor size was larger (mean volume: $381 \pm 296\ mm^3$ on day 63) 2 months after the injection in the $Z_{HER2:342}$-Cupid-His-Ax-SiPc

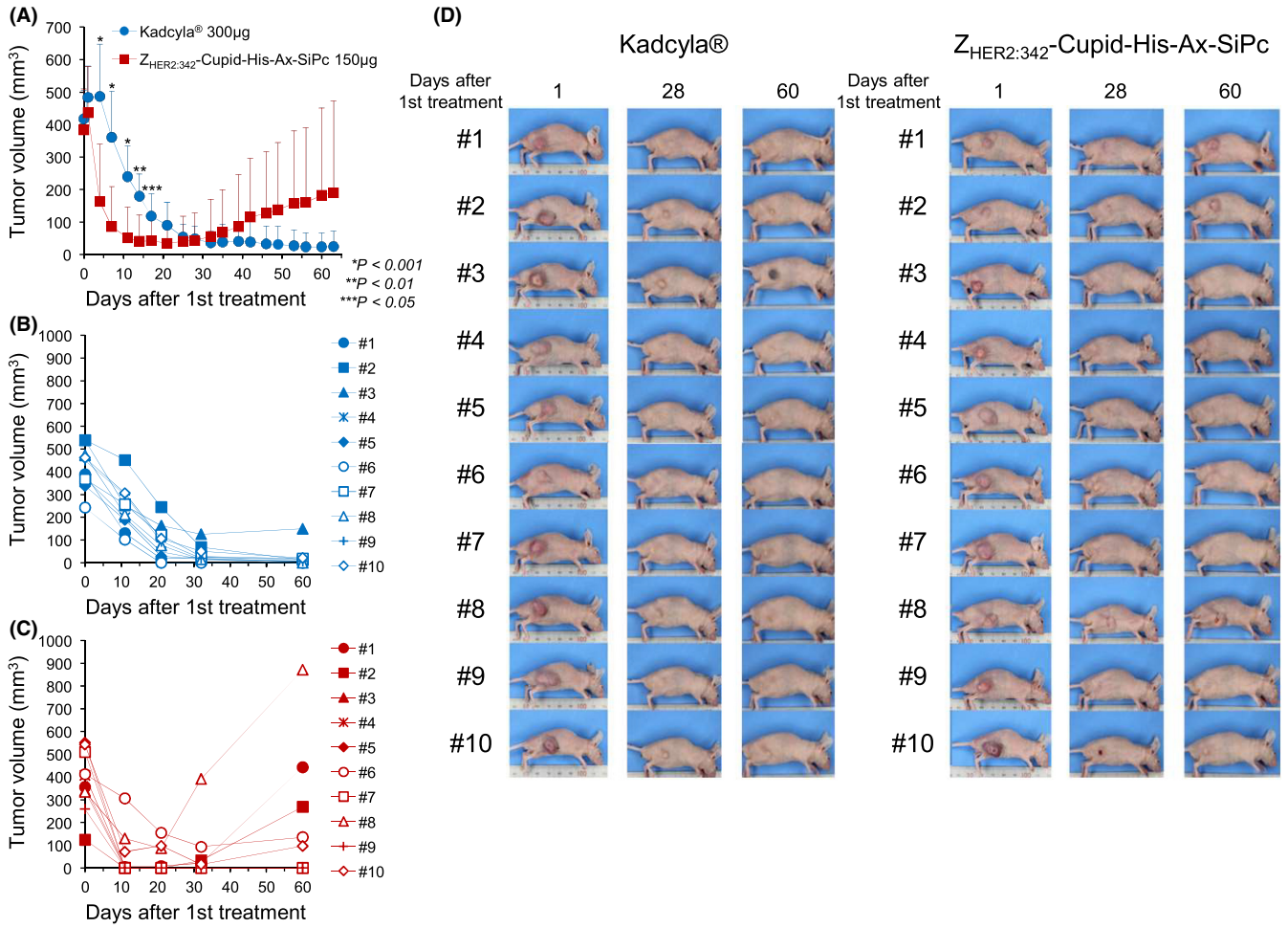

FIGURE 2 Tumor volumes before and after the single-dose treatment. (A) Tumor growth curve of the Kadcyla group (300 μg/body, solid circle) and $Z_{HER2:342}$-Cupid-His-Ax-SiPc group (150 μg/body, solid square). (B) The individual tumor growth curve of the Kadcyla group ($n = 10$). (C) The individual tumor growth curve of the $Z_{HER2:342}$-Cupid-His-Ax-SiPc group ($n = 10$). (D) Representative animals with tumors after the single-dose treatment (left panel; Kadcyla group, right panels; $Z_{HER2:342}$-Cupid-His-Ax-SiPc group)

group, whereas a steady decrease in tumor size was observed in the Kadcyla® group. These data suggest that short-term local AMDC treatment has strong antitumor effects against HER2-positive breast cancer but could lead to tumor relapse after the first treatment in some cases.

3.2 | Second local AMDC treatment rapidly reduced and completely eradicated relapsed tumors

In order to examine the efficacy of repeated local AMDC treatment, $Z_{HER2:342}$-Cupid-His-Ax-SiPc pre-conjugate was injected into the xenograft model mice on day 63 after the first treatment (44 days after the tumor observation period), and the relapsed tumor size was measured. Figure 3 shows the change in size of the five tumor relapse cases after the second $Z_{HER2:342}$-Cupid-His-Ax-SiPc treatment. The tumor volume in the xenograft model mice decreased more rapidly after the second $Z_{HER2:342}$-Cupid-His-Ax-SiPc treatment as compared with that after the first $Z_{HER2:342}$-Cupid-His-Ax-SiPc treatment. Furthermore, the tumors disappeared in all mice 7 days after the second $Z_{HER2:342}$-Cupid-His-Ax-SiPc injection (Figure 3A,B), and no regrowth was noted even more than 1 month after the second $Z_{HER2:342}$-Cupid-His-Ax-SiPc treatment. There was a significant difference in tumor size between day 0 and day 97 after the first $Z_{HER2:342}$-Cupid-His-Ax-SiPc treatment. Additionally, the lump size in the repeated $Z_{HER2:342}$-Cupid-His-Ax-SiPc treatment group became smaller to the same level as the Kadcyla® treatment group, 97 days after the first treatment (Figure 3C). These results suggest that the repeated local AMDC treatment rapidly and completely resolved the relapsed tumors.

3.3 | Local AMDC treatment had a robust effect on the HER2-positive xenograft tumor models without causing skin degeneration

In order to assess the pathological response to the local AMDC treatment, we conducted a histological examination of the tissues in KPL-4 xenograft model mice on day 97 after Kadcyla® and $Z_{HER2:342}$-Cupid-His-Ax-SiPc treatment. Histologically, no remaining

tumor cells were observed in any of the Kadcyla®-treated ($n = 10$) or second AMDC-treated ($n = 10$) mice in the subcutaneous regions around the xenografted KPL-4 tumor sites on day 97 (Figure 4, S3). To the best of our knowledge, there were no metastatic tumors in the lymph nodes or distant organs in any of the mice (Figure 4). Thus, it was concluded that pathological complete remission was achieved in both groups. Further histological observations showed that granulomatous reactions with the nests of hemosiderin-laden macrophages and/or focal calcifications were frequently observed in the subcutaneous regions of the Kadcyla®-treated mice (6/10 [mouse #1, 2, 3, 7, 8, and 10], 60%) (Figure 4). In one of the Kadcyla®-treated mice (mouse #2), a subcutaneous cyst surrounded by granulomatous tissue was also noted. In contrast, these granulomatous reactions were rarely observed in the AMDC-treated group (1/10 [mouse #6], 10%) (Figure 4) ($p < 0.001$, chi-squared test). After the second local AMDC treatment, pathological complete remission of the xenografted KPL-4 tumors was clearly achieved. Moreover, no histologically obvious side effects were observed in the vital organs, except for microscopic focal liver necroses observed in two of the mice (mouse # 2 and 6) (Figure 4).

Furthermore, we measured chronological changes in xenograft body weight after Kadcyla® and $Z_{HER2:342}$-Cupid-His-Ax-SiPc treatment. The body weights of the xenograft model mice after Kadcyla® treatment showed moderately increasing trends among all individual mice (Figure 5A). One xenograft $Z_{HER2:342}$-Cupid-His-Ax-SiPc–treated mouse among the tumor relapse cases lost weight 3 weeks

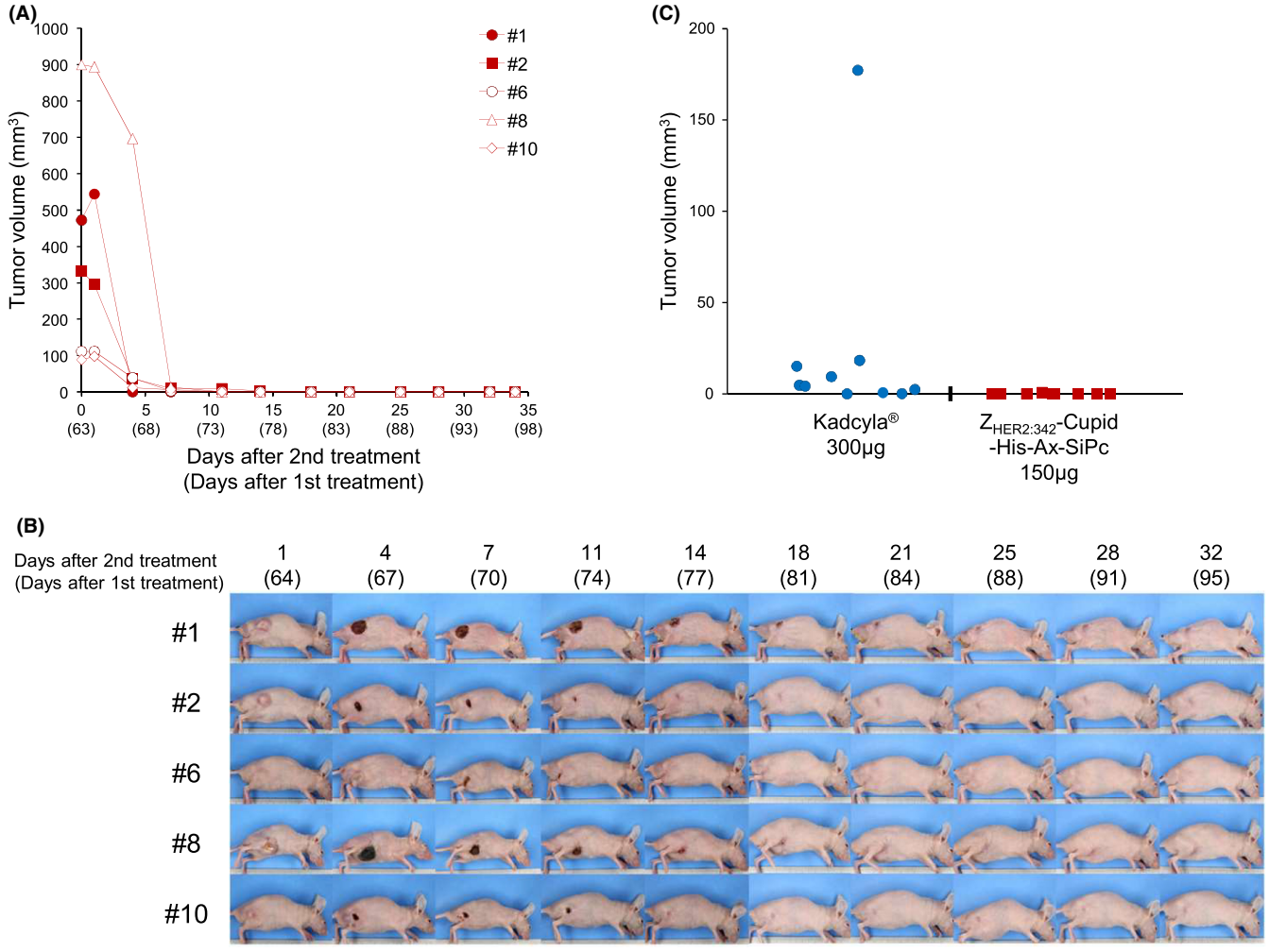

FIGURE 3 The second-dose treatment of $Z_{HER2:342}$-Cupid-His-Ax-SiPc in the recurrence group. (A) Tumor growth curve after the second treatment using the same dosage as the first treatment (150 μg/body and two times light irradiation). (B) Tumor growth curve of the recurrence group mice from day 1 to day 32 after the second treatment. (C) Individual tumor volume of the Kadcyla group (solid circle) and $Z_{HER2:342}$-Cupid-His-Ax-SiPc group (solid square) on day 97

FIGURE 4 Effect of the tumor eradications by the $Z_{HER2:342}$-Cupid-His-Psyche-Ax-SiPc complex in histopathological examinations. Histopathological analysis of the skin and major organ tissues (liver, kidney, and lung) in the xenograft model mice on day 97 after Kadcyla and $Z_{HER2:342}$-Cupid-His-Psyche-Ax-SiPc treatments. The black scale bar with value (μm) in each picture indicates the size of histological picture

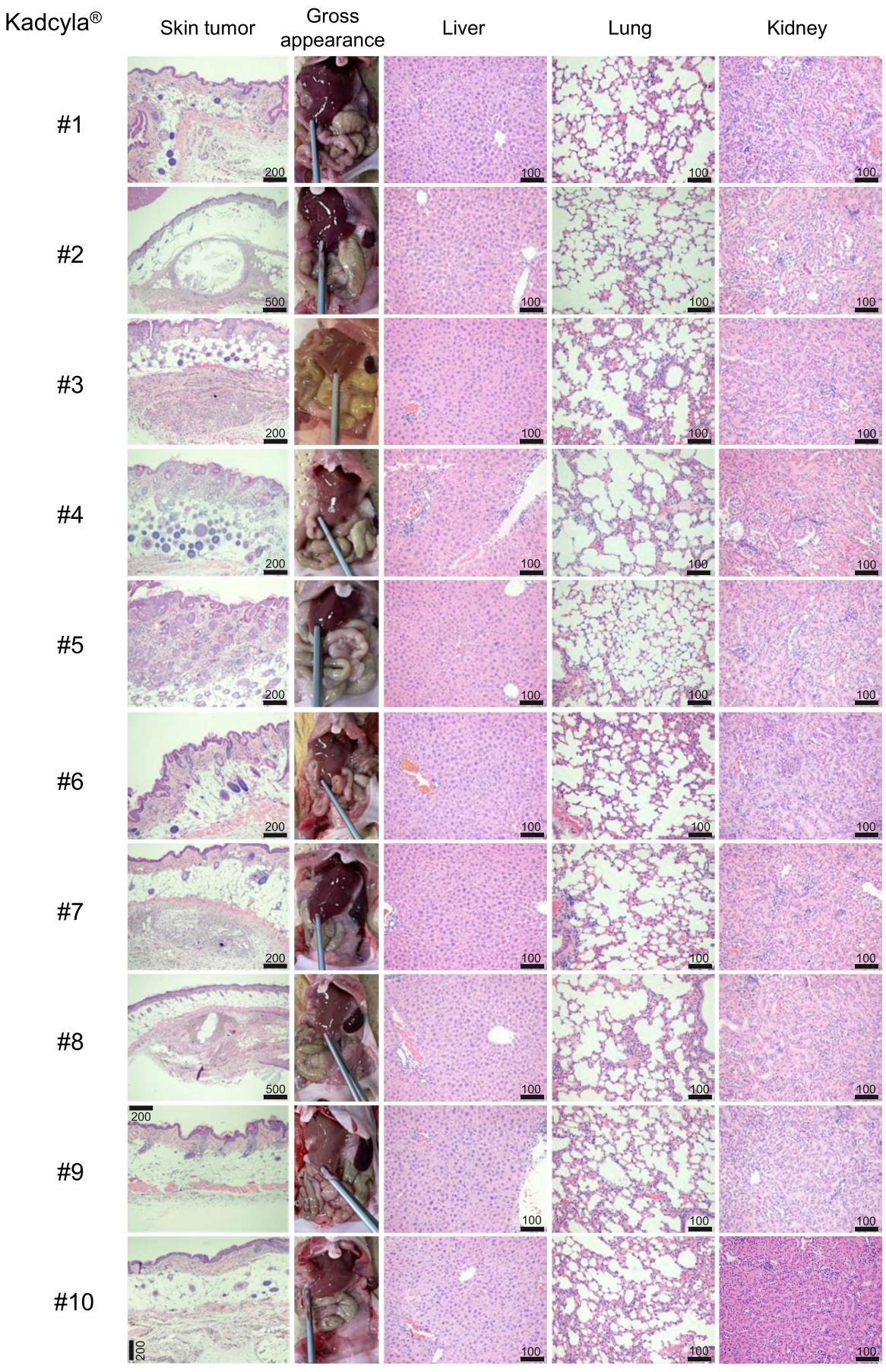
Kadcyla®
Skin tumor
Gross appearance
Liver
Lung
Kidney
#1
#2
#3
#4
#5
#6
#7
#8
#9
#10
200
500
100

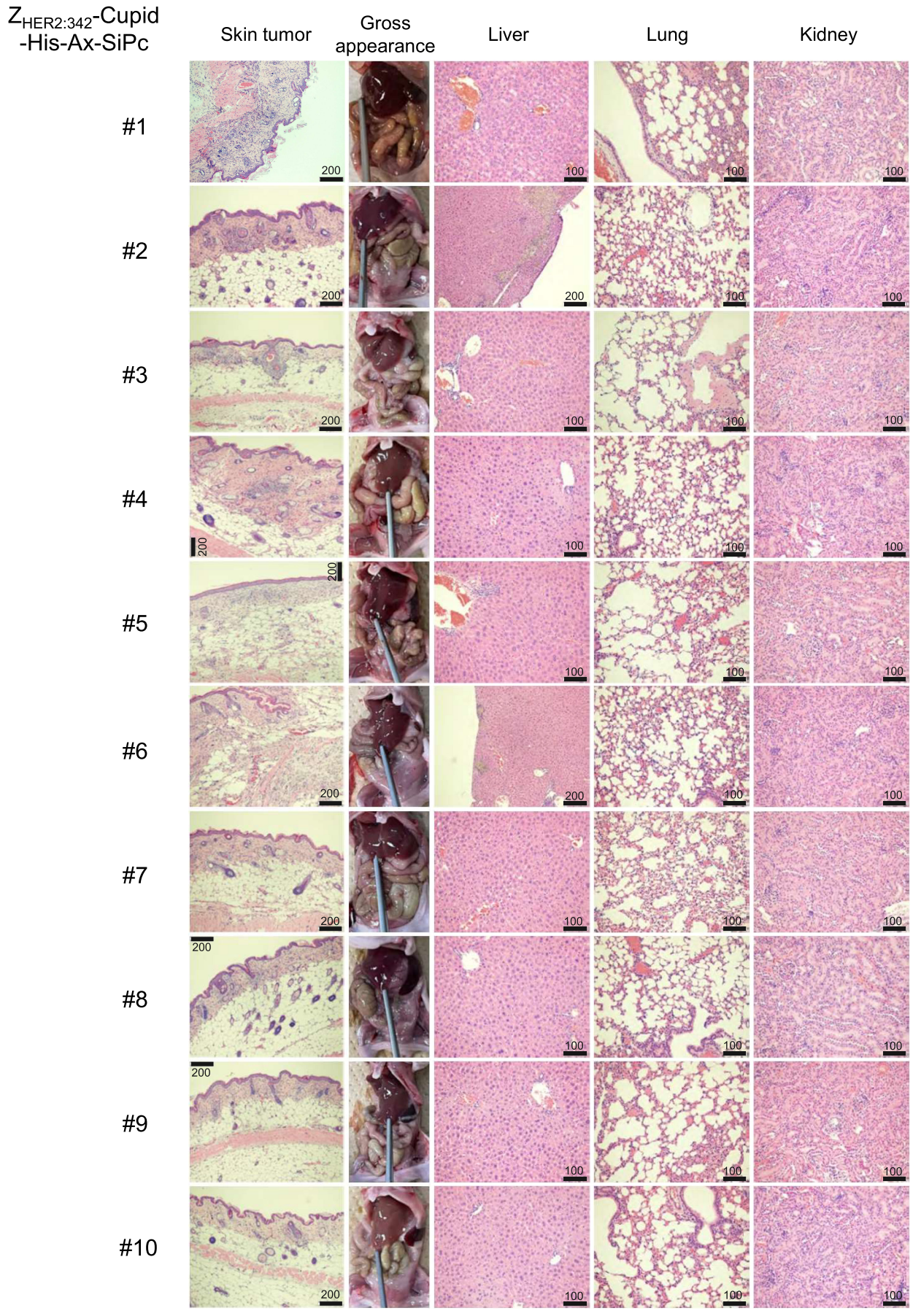

FIGURE 4 (Continued)

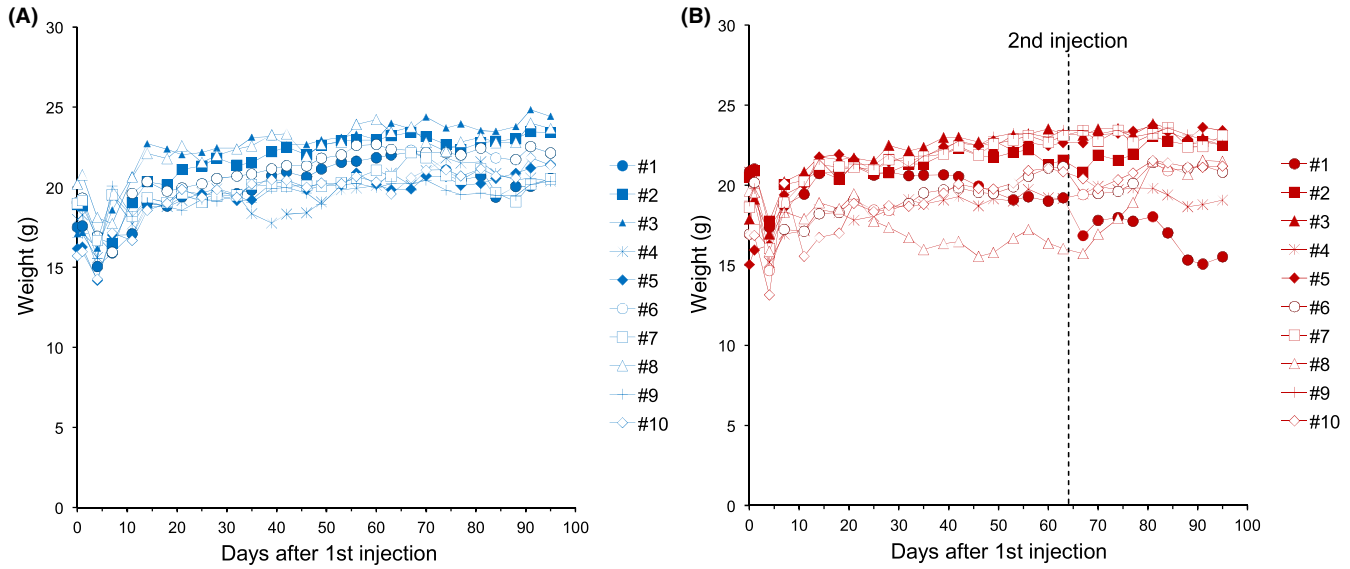

FIGURE 5 Timeline of the individual weight of the mice in the Kadcyla group (A) and $Z_{HER2:342}$-Cupid-His-Ax-SiPc group (B) after the first treatment. In Figure 5B, dotted line shows the day on which the $Z_{HER2:342}$-Cupid-His-Ax-SiPc second treatment was performed

after the first treatment but rapidly gained weight after the second treatment (Figure 5B). Another xenograft $Z_{HER2:342}$-Cupid-His-Ax-SiPc–treated mouse among the recurrence cases lost weight even after the second treatment, which could be attributed to an unrelated infectious disease coincidentally found during histopathological examination. These data indicate that local AMDCs have a robust therapeutic effect on the xenograft model with few side effects.

4 | DISCUSSION

4.1 | Efficacy of repeated photo-activating AMDC against relapsed tumor

Recently, we reported an animal experiment using photo-activating AMDC against HER2-expressing xenograft tumor,[11,12] where all KPL-4 xenografted tumors were rapidly eradicated macroscopically after treatment but the pathological study revealed that one in three animals showed remaining clusters of malignant cells. This may cause problems in the long-term efficacy of AMDCs. Expanding clinical experience with HER2-targeting antibody therapy and ADC against solid tumors also showed that intrinsic and acquired resistance to these therapies limits their long-term efficacy.[17,25,26]

The present study was designed to clarify whether repeated AMDC treatment can achieve complete remission. For this purpose, the condition for a higher probability of relapse in KPL-4, a HER2-expressing human breast cancer cell, was selected. Usually, KPL-4 tumors were treated when they reach 200-300 mm^3 in size.[27] If tumors become larger, penetration of near infrared light may become insufficient,[28,29] or the drug concentration in parts of large tumors may not be sufficient. In this study, we selected mice with larger tumors (approximately 400 mm^3) at the start of treatment. Photo-activating AMDC treatment rapidly induced shrinkage of all tumors, but during the 40 days of the observation period, 5 out of 10 treated mice developed relapsed tumors macroscopically (Figures 2, 3).

Further, we started repeated treatment when the size of the relapsed tumors reached nearly the original tumor size to evaluate the efficacy of repeated treatment. All tumors were eradicated macroscopically, and histological analysis revealed pathological complete remission (Figure 4, S3). Histological studies of the remaining five mice without relapsing tumors also showed pathological complete remission. Unexpectedly, unlike the initial treatment results, all mice treated twice showed pathological complete remission. Except for minor liver injury, the mice tolerated the repeated treatment well. These results suggest that repeated photo-activating AMDC treatment effectively eradicates xenograft tumors.

4.2 | Mechanism of pathological complete remission by repeated treatment

The sophisticated molecular design of photo-activating AMDCs enables rapid and accurate killing of cancer cells. The anti-HER2 AMDC contains four molecules of a high-affinity HER2-binding affibody, $Z_{HER2:342}$, which has an extraordinarily high affinity for HER2 (22 pM) as a monomer.[11,13] As a tetramer, it shows very high avidity against HER2-expressing tumor cells, maintaining the stable state of binding to the target tumor cells.[11] Furthermore, our AMDCs bound to normal tissues could be washed out in 20-hour intervals between the drug injection and light irradiation, enhancing our AMDCs' specificity for the target tumors. The anti-HER2 AMDC, formally $Z_{HER2:342}$-Cupid-His-Ax-SiPc, is based on the mutant streptavidin (Cupid) and bis-iminobiotin (Psyche) systems.[12] Each anti-HER2 AMDC tetrameric complex contained two highly functional Ax-SiPc molecules. Upon near-infrared activation, each Ax-SiPc can generate 1.5-fold more singlet oxygen than the current IR700.[13] Therefore,

the cytotoxic activity of our AMDCs is dependent on the light irradiation and drug concentration.[11] As shown in our previous and current studies, photo-activating anti-HER2 AMDC strictly binds to the cell surface of HER2-expressing cells, which preserves the surrounding normal skin tissue and innate immune cells.[11] In a clinical setting, when most malignant cells get killed rapidly, genetically mutated proteins and other cancer-specific target molecules could be exposed to the surrounding immune cells. This would increase the possibility of enhanced immunity against tumor cells.[30] A similar effect has been reported for photoimmunotherapy using IR700 against EGFR.[31] They observed that photoimmunotherapy caused rapid and irreversible damage to the cell membrane, leading to swelling, bursting, and release of intracellular components due to the influx of water into the cell. This process also induces the relocation of immunologic cell death markers to the cell surface and the rapid release of immunogenic signals, followed by the maturation of dendritic cells.[32] CD44-targeted photoimmunotherapy has been reported to induce infiltration of CD8+ cells.[22] These results suggest that enhanced tumor-associated immunity such as innate immunity by rapid and selective destruction of malignant cells after initial treatment may be an important mechanism for unexpected pathological complete remission after repeated photo-activating AMDC treatment.

We speculate that the initial photo-activating AMDC treatment caused the rapid reduction in tumor cells mainly by the physicochemical mechanism of singlet oxygen. The tumor size in the AMDC treatment group was reduced to approximately half of its original size within 4 days, compared with 14 days in the Kadcyla® treatment group, which was used as a control ADC (Figures 2, 3). Rapidly dying cancer cells may evoke tumor immunity, which enhances tumor killing in repeated treatments.[30] In this study, we used a nude mouse strain to evaluate anti-human HER2 treatment using the $Z_{HER2:342}$-AMDC system. Nude mice lack T cell immunity but sustain intact innate immunity and, although insufficient, humoral immunity[33]; thus, our model may provide clues to investigate the possible immunological mechanisms by which the second AMDC treatment could rapidly achieve pathological complete remission. To fully investigate the immunological reactions to AMDC treatment during the first and second rapid killing of tumors, humanized HER2+ mouse tumor models[34] may be suitable candidates for our $Z_{HER2:342}$-AMDC system. The rapid achievement of pathological complete remission, without pathological granulomatous regeneration in our second AMDC-treated model, may provide a new aspect of tumor-associated innate immunity. The remaining or leaked immunity in the FOXN1-deficient nude mice has been analyzed intensively,[32,35] and further investigation is needed to consider possible immunological reactions in this mouse strain.

4.3 | Rapid healing and minimal side effect: Perspective for repeated therapy

In this study, the rapid eradication of malignant tumors may have caused severe damage to the tumor tissues. The black color of the tumor tissues (Figures 2, 3) suggests that severe damage occurred. However, after 20 days, the lesions healed rapidly. Pathological examination revealed appropriate regeneration of damaged subcutaneous tissues in the mice. It was considered that the photo-activating AMDCs can act only against malignant cells and preserve normal skin tissue, and the regenerative reactions may enable rapid restorations (Figure 4). In this study, this rapid healing of the damaged tissues after initial treatment,[11] as well as recovery after relapsed tumors by repeated $Z_{HER2:342}$-Cupid-His-Ax-SiPc therapy, support the efficacy and safety of repeated treatment.

In addition to local healing after photo-activating AMDCs, no serious macroscopic changes have been noted in other organs, except for microscopic granulomatous foci beneath the anterior serosa of the liver in a few mice. In animal studies, due to limited shielding of near-infrared irradiation, some parts of the liver surface were irradiated by leaked light through the extremely thin skin of the mice. The liver is known to accumulate the highest amount of unbound AMDC drugs and antibody-Cupid complex,[11,12] which can be avoided by the extension of the interval between the injection and irradiation. The activated photo absorber, Ax-SiPc, may generate a singlet oxygen molecule beneath the serous membrane,[13] which may cause tissue injury. The damaged cells can be cleared by macrophages, causing foci of hemosiderin-laden macrophages and granulomatous lesions (Figure 4). In human clinical settings, the liver should be adequately shielded in future clinical photo-activating AMDCs.

A global phase III clinical trial of photoimmunotherapy for unresectable head and neck cancers is currently in progress.[21] Patients with vulvar Paget's disease face difficulties in surgical operations due to the involvement of sensitive organs, including sex organs, urethra, and anus. Difficulties in identifying the margins of creeping tumors and relapse after surgery may worsen patients' quality of life.[36,37] A recent genome-wide analysis revealed that HER2 amplification and mutation are significant driver mutations in extramammary Paget's disease.[38] These results suggest that repeated treatment using anti-HER2 photo-activating AMDCs may be a suitable therapeutic regimen for the treatment of vulvar Paget's disease, in combination with other therapeutic modalities including chemotherapy, radiation therapy, hormone therapy, and immune checkpoint inhibitors or other immunomodulators.[18,39] In addition, when combined with endoscopic tools, the therapies of the AMDC with photosensitizers would possibly be applicable to various malignancies in the gastrointestinal tracts.[40,41] In some clinical cases, tumor cells may have already spread outside of the primary sites even at the early stages; in those cases, the AMDC with photosensitizer treatment which targets local tumors would harbor disadvantages. However, it is notable that among patients with vulvar Paget's disease, only a few cases show metastases at the time of diagnosis,[42] confirming that it is a good candidate for the targets of this therapy. This study and previous studies suggest that repeated photo-activating AMDC treatment may achieve complete remission of targeted tumors.[11,12] Resistance to the current ADC regimen is considered to be caused by intratumor heterogeneity of genetic mutation development of resistance to the specific payload.[18,19,26,27,43]

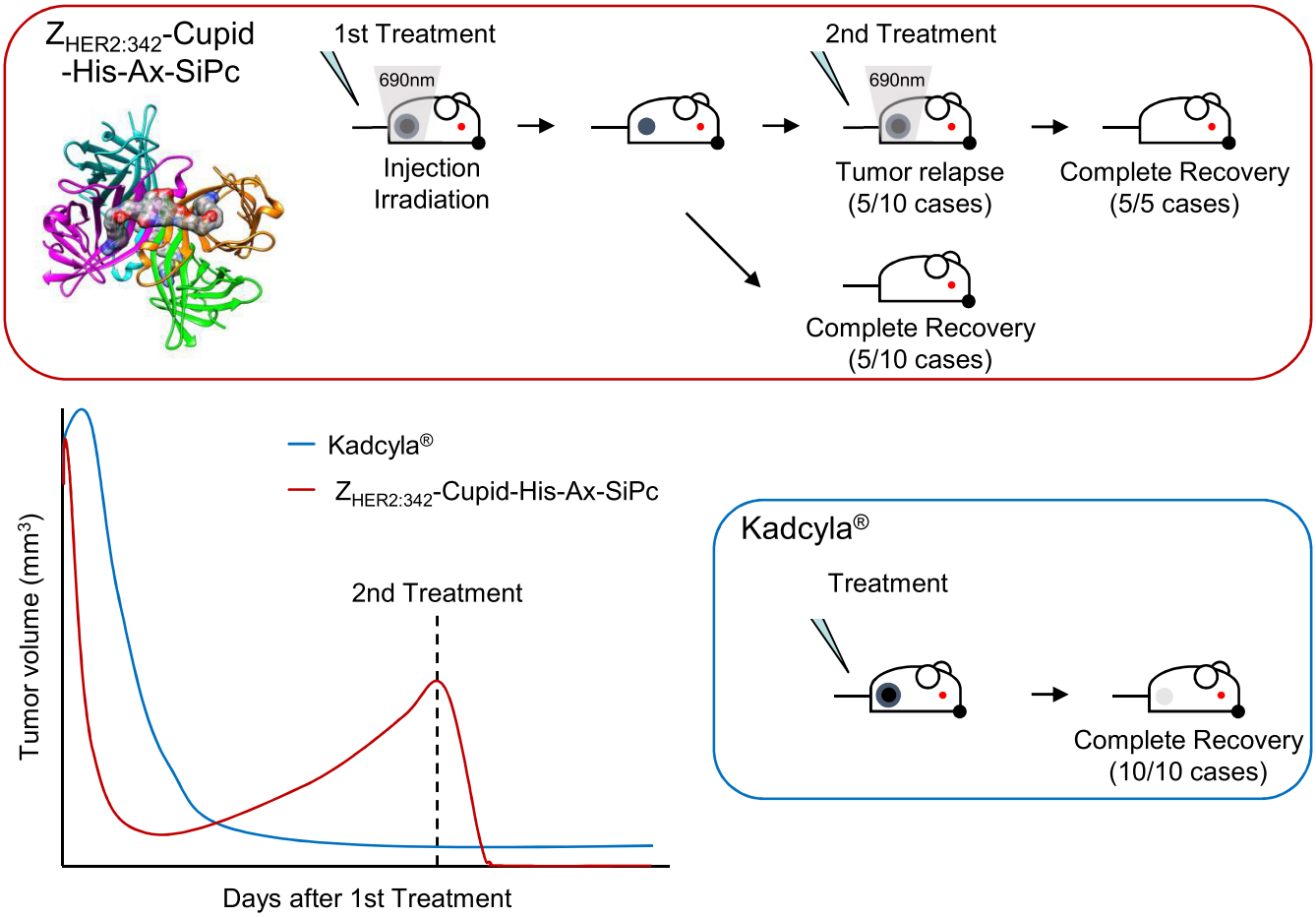

FIGURE 6 Schematic summary of this study. Photo-activating antibody–mimetic drug conjugate ($Z_{HER2:342}$-Cupid-His-Ax-SiPc) treatment reduces the tumors in the HER2-positive xenograft tumor model rapidly. Repeated treatment using photo-activating antibody–mimetic drug conjugate has completely resolved the relapsed tumors in the recurrence cases with few side effects

AMDCs can provide a wide range of antibody-mimetics for target heterogeneity and various kinds of payload, which can be easily conjugated by noncovalent conjugation by simply mixing prior to use. Further studies on the precise nature of the possible induction of tumor immunity may further enhance the therapeutic efficacy of photo-activating AMDCs.

We acknowledge there are several limitations to this study. First, we were unable to analyze the differences between mice in which the tumors disappeared and relapsed. Second, due to the use of a nude mouse model, we could not clearly conclude whether immune responses by the first AMDC treatment potentiated the second AMDCs' therapeutic effects. To this end, we need to analyze immune responses and histological examination in the middle of the AMDC treatments in other mouse models with proper immune systems. It would also be necessary to investigate various HER2-overexpressing cell lines in vivo to further generalize our observation.

In conclusion, we have established a relapse xenograft tumor model, and our results indicated the potential therapeutic efficacy of the repeated photo-activating AMDC treatment against tumors, leading to the establishment of further effective cancer therapy (Figure 6).

ACKNOWLEDGMENTS

We thank Mr. Osayasu Kikuchi and Mr. Masatoshi Tsuchiya (Yamato Scientific Co., Ltd.) for providing a 690-nm light source.

FUNDING INFORMATION

This work was supported by the Japan Society for the Promotion of Science (JSPS KAKENHI, Grant number JP21392851 [to A. Sugiyama]); the Japan Agency for Medical Research and Development (AMED, Grant number JP20ck0106414 [to T. Kodama], JP21am0401010 [to S. Ishikawa], and JP21ak0101096 [to H. Katoh]); the Takeda Science Foundation, Japan and Kowa Life Science Foundation, Japan [to K. Yamatsugu]; and the Program for Promoting Research on the Supercomputer Fugaku (JPMXP1020200201, hp210172) [to T. Yamashita]. This work was also supported by Savid Therapeutics, Inc.

DISCLOSURE

Y.K. is an employee of Medical & Biological Laboratories Co., Ltd.; T.T. has a sponsored research agreement from Savid Therapeutics, Inc.; M.T. and C.M. are board members of Savid Therapeutics, Inc.; M.T., T.K., and A.S. are cofounders of Savid Therapeutics, Inc; S.I. and

H.K. possess latent profit of stock option from Savid Therapeutics, Inc; and S.I. is an editorial board member of *Cancer Science*. Other authors have no conflict of interest to declare.

ETHICS STATEMENT

Approval of the research protocol by an Institutional Reviewer Board: N/A.

Informed Consent: N/A.

Registry and the Registration No. of the study/trial: N/A.

Animal Studies: This research was approved by the Institutional Animal Care and Use Committee (approval number: RAC210005) and performed according to the animal experimentation regulations of the University of Tokyo.

ORCID

Yudai Kaneko https://orcid.org/0000-0003-0967-782X
Akira Sugiyama https://orcid.org/0000-0003-4406-9475
Hiroto Katoh https://orcid.org/0000-0001-9440-728X

REFERENCES

1. Chari RV, Miller ML, Widdison WC. Antibody-drug conjugates: an emerging concept in cancer therapy. *Angew Chem Int Ed Engl*. 2014;53(14):3796-3827. doi:10.1002/anie.201307628
2. Panowski S, Bhakta S, Raab H, Polakis P, Junutula JR. Site-specific antibody drug conjugates for cancer therapy. *MAbs*. 2014;6(1):34-45. doi:10.4161/mabs.27022
3. Senter PD. Potent antibody drug conjugates for cancer therapy. *Curr Opin Chem Biol*. 2009;13(3):235-244. doi:10.1016/j.cbpa.2009.03.023
4. Lee YT, Tan YJ, Oon CE. Molecular targeted therapy: treating cancer with specificity. *Eur J Pharmacol*. 2018;834:188-196. doi:10.1016/j.ejphar.2018.07.034
5. Chia CSB. A patent review on FDA-approved antibody-drug conjugates, their linkers and drug payloads. *ChemMedChem*. 2022;17(11):e202200032. doi:10.1002/cmdc.202200032
6. Verhaar ER, Woodham AW, Ploegh HL. Nanobodies in cancer. *Semin Immunol*. 2021;52:101425. doi:10.1016/j.smim.2020.101425
7. Stahl S, Graslund T, Eriksson Karlstrom A, Frejd FY, Nygren PA, Lofblom J. Affibody molecules in biotechnological and medical applications. *Trends Biotechnol*. 2017;35(8):691-712. doi:10.1016/j.tibtech.2017.04.007
8. Crook ZR, Nairn NW, Olson JM. Miniproteins as a powerful modality in drug development. *Trends Biochem Sci*. 2020;45(4):332-346. doi:10.1016/j.tibs.2019.12.008
9. David A, Islam S, Tankhilevich E, Sternberg MJE. The AlphaFold database of protein structures: a biologist's guide. *J Mol Biol*. 2022;434(2):167336. doi:10.1016/j.jmb.2021.167336
10. Huang PS, Boyken SE, Baker D. The coming of age of de novo protein design. *Nature*. 2016;537(7620):320-327. doi:10.1038/nature19946
11. Yamatsugu K, Katoh H, Yamashita T, et al. Antibody mimetic drug conjugate manufactured by high-yield *Escherichia coli* expression and non-covalent binding system. *Protein Expr Purif*. 2022;192:106043. doi:10.1016/j.pep.2021.106043
12. Sugiyama A, Kawamura T, Tanaka T, et al. Cupid and Psyche system for the diagnosis and treatment of advanced cancer. *Proc Jpn Acad Ser B Phys Biol Sci*. 2019;95(10):602-611. doi:10.2183/pjab.95.041
13. Takahashi K, Sugiyama A, Ohkubo K, et al. Axially substituted silicon phthalocyanine payloads for antibody-drug conjugates. *Synlett*. 2021;32(11):1098-1103. doi:10.1055/a-1503-6425
14. Tolmachev V, Nilsson FY, Widstrom C, et al. 111In-benzyl-DTPA-ZHER2:342, an affibody-based conjugate for in vivo imaging of HER2 expression in malignant tumors. *J Nucl Med*. 2006;47(5):846-853.
15. Siavoshinia L, Kheirollah A, Zeinali M, Barzegari E, Jamalan M. Combinatorial in silico and in vivo evaluation of immune response elicitation by the affibody ZHER2. *Int Immunopharmacol*. 2021;101:108368. doi:10.1016/j.intimp.2021.108368
16. Tarcsa E, Guffroy MR, Falahatpisheh H, Phipps C, Kalvass JC. Antibody-drug conjugates as targeted therapies: are we there yet? A critical review of the current clinical landscape. *Drug Discov Today Technol*. 2020;37:13-22. doi:10.1016/j.ddtec.2020.07.002
17. Baah S, Laws M, Rahman KM. Antibody-drug conjugates-A tutorial review. *Molecules*. 2021;26(10):2943. doi:10.3390/molecules26102943
18. Goutsouliak K, Veeraraghavan J, Sethunath V, et al. Towards personalized treatment for early stage HER2-positive breast cancer. *Nat Rev Clin Oncol*. 2020;17(4):233-250. doi:10.1038/s41571-019-0299-9
19. Zimmer AS, Denduluri N. When to add additional anti-HER2 therapy to adjuvant trastuzumab. *Curr Oncol Rep*. 2019;21(12):109. doi:10.1007/s11912-019-0848-5
20. Mitsunaga M, Ogawa M, Kosaka N, Rosenblum LT, Choyke PL, Kobayashi H. Cancer cell-selective in vivo near infrared photoimmunotherapy targeting specific membrane molecules. *Nat Med*. 2011;17(12):1685-1691. doi:10.1038/nm.2554
21. Maruoka Y, Wakiyama H, Choyke PL, Kobayashi H. Near infrared photoimmunotherapy for cancers: a translational perspective. *EBioMedicine*. 2021;70:103501. doi:10.1016/j.ebiom.2021.103501
22. Wakiyama H, Furusawa A, Okada R, et al. Increased immunogenicity of a minimally immunogenic tumor after cancer-targeting near infrared photoimmunotherapy. *Cancers (Basel)*. 2020;12(12):3747. doi:10.3390/cancers12123747
23. Kurebayashi J, Otsuki T, Tang CK, et al. Isolation and characterization of a new human breast cancer cell line, KPL-4, expressing the Erb B family receptors and interleukin-6. *Br J Cancer*. 1999;79(5–6):707-717. doi:10.1038/sj.bjc.6690114
24. Lambert JM, Chari RV. Ado-trastuzumab Emtansine (T-DM1): an antibody-drug conjugate (ADC) for HER2-positive breast cancer. *J Med Chem*. 2014;57(16):6949-6964. doi:10.1021/jm500766w
25. Tesch ME, Gelmon KA. Targeting HER2 in breast cancer: latest developments on treatment sequencing and the introduction of biosimilars. *Drugs*. 2020;80(17):1811-1830. doi:10.1007/s40265-020-01411-y
26. Kay C, Martinez-Perez C, Meehan J, et al. Current trends in the treatment of HR+/HER2+ breast cancer. *Future Oncol*. 2021;17(13):1665-1681. doi:10.2217/fon-2020-0504
27. Fujimoto-Ouchi K, Sekiguchi F, Yamamoto K, Shirane M, Yamashita Y, Mori K. Preclinical study of prolonged administration of trastuzumab as combination therapy after disease progression during trastuzumab monotherapy. *Cancer Chemother Pharmacol*. 2010;66(2):269-276. doi:10.1007/s00280-009-1160-0
28. Ji Y, Jones C, Baek Y, Park GK, Kashiwagi S, Choi HS. Near-infrared fluorescence imaging in immunotherapy. *Adv Drug Deliv Rev*. 2020;167:121-134. doi:10.1016/j.addr.2020.06.012
29. Matsuoka K, Sato M, Sato K. Hurdles for the wide implementation of photoimmunotherapy. *Immunotherapy*. 2021;13(17):1427-1438. doi:10.2217/imt-2021-0241
30. Kobayashi H, Furusawa A, Rosenberg A, Choyke PL. Near-infrared photoimmunotherapy of cancer: a new approach that kills cancer cells and enhances anti-cancer host immunity. *Int Immunol*. 2021;33(1):7-15. doi:10.1093/intimm/dxaa037
31. Ogawa M, Tomita Y, Nakamura Y, et al. Immunogenic cancer cell death selectively induced by near infrared photoimmunotherapy initiates host tumor immunity. *Oncotarget*. 2017;8(6):10425-10436. doi:10.18632/oncotarget.14425

32. Romano R, Palamaro L, Fusco A, et al. FOXN1: a master regulator gene of thymic epithelial development program. *Front Immunol*. 2013;4:187. doi:10.3389/fimmu.2013.00187
33. Kelland LR. Of mice and men: values and liabilities of the athymic nude mouse model in anticancer drug development. *Eur J Cancer*. 2004;40(6):827-836. doi:10.1016/j.ejca.2003.11.028
34. Piechocki MP, Ho YS, Pilon S, Wei WZ. Human ErbB-2 (Her-2) transgenic mice: a model system for testing Her-2 based vaccines. *J Immunol*. 2003;171(11):5787-5794. doi:10.4049/jimmunol.171.11.5787
35. Liebman MA, Roche MI, Williams BR, Kim J, Pageau SC, Sharon J. Antibody treatment of human tumor xenografts elicits active anti-tumor immunity in nude mice. *Immunol Lett*. 2007;114(1):16-22. doi:10.1016/j.imlet.2007.08.006
36. Preti M, Micheletti L, Borella F, et al. Vulvar Paget's disease and stromal invasion: c linico-pathological features and survival outcomes. *Surg Oncol*. 2021;38:101581. doi:10.1016/j.suronc.2021.101581
37. Matsuo K, Nishio S, Matsuzaki S, et al. Surgical margin status and recurrence pattern in invasive vulvar Paget's disease: a Japanese gynecologic oncology group study. *Gynecol Oncol*. 2021;160(3):748-754. doi:10.1016/j.ygyno.2020.12.023
38. Ishida Y, Kakiuchi N, Yoshida K, et al. Unbiased detection of driver mutations in extramammary Paget disease. *Clin Cancer Res*. 2021;27(6):1756-1765. doi:10.1158/1078-0432.CCR-20-3205
39. Kato T, Okada R, Furusawa A, et al. Simultaneously combined cancer cell- and CTLA4-targeted NIR-PIT causes a synergistic treatment effect in syngeneic mouse models. *Mol Cancer Ther*. 2021;20(11):2262-2273. doi:10.1158/1535-7163.MCT-21-0470
40. Okuyama S, Nagaya T, Sato K, et al. Interstitial near-infrared photoimmunotherapy: effective treatment areas and light doses needed for use with fiber optic diffusers. *Oncotarget*. 2018;9(13):11159-11169. doi:10.18632/oncotarget.24329
41. Maruoka Y, Nagaya T, Sato K, et al. Near infrared photoimmunotherapy with combined exposure of external and interstitial light sources. *Mol Pharm*. 2018;15(9):3634-3641. doi:10.1021/acs.molpharmaceut.8b00002
42. Yoshino K, Kiyohara T, Sakasegawa J, et al. Skin cancer guideline version 3, medical treatment guideline the vulvar Paget's disease in 2021. *JPN Dermatol Assoc*. 2021;131(2):225-244.
43. Koganemaru S, Shitara K. Antibody-drug conjugates to treat gastric cancer. *Expert Opin Biol Ther*. 2021;21(7):923-930. doi:10.1080/14712598.2020.1802423

SUPPORTING INFORMATION

Additional supporting information can be found online in the Supporting Information section at the end of this article.

How to cite this article: Kaneko Y, Yamatsugu K, Yamashita T, et al. Pathological complete remission of relapsed tumor by photo-activating antibody–mimetic drug conjugate treatment. *Cancer Sci*. 2022;00:1-13. doi: 10.1111/cas.15565